Molecular adsorption and multilayer growth of pentacene on Cu(100): Layer structure and energetics

M. Satta,[1,2] S. Iacobucci,[1] and R. Larciprete[1]
[1]*CNR, Institute of Complex Systems, Sez. Montelibretti, Via Salaria, Km. 29.3; 00016 Monterotondo Scalo (RM), Italy*
[2]*Dipartimento di Fisica dell'Università di Roma "La Sapienza," Piazzale Aldo Moro 5, 00185 Roma, Italy*
(Received 16 October 2006; revised manuscript received 10 January 2007; published 2 April 2007)

We used the partial charge tight binding method to perform a full structure optimization to determine equilibrium adsorption geometries, energetics, and local charge redistribution for molecular adsorption and multilayer growth of pentacene on Cu(100). We found that single molecule adsorption induces only a localized perturbation of the metal lattice which is limited to the topmost layers. At saturation coverage four stable topologies (Brick, Wave, Lines and Zigzag) were identified, all based on pentacene molecules lying flat on the metal surface and with the central phenyl ring adsorbed in top position. Only two (Brick and Wave) out of the four structures are able to sustain multilayer growth. In both cases, assembling beyond the second layer corresponds to a transition from the flat to a tilted geometry, in which the pentacenes adopt a face-plane-face arrangement leading to a herringbone structure. The energetics of the different structure are reported as a function of the molecular number density of the pentacene multilayer by calculating cohesive, stress, and electrostatic energies. The dominant tilted molecular orientation in the pentacene multilayer is in agreement with the average tilt angle of 65° between the molecular plane and the Cu surface derived by near edge x-ray absorption spectroscopy of a four monolayer pentacene film deposited on Cu(100).

DOI: 10.1103/PhysRevB.75.155401 PACS number(s): 68.35.−p, 68.43.Fg, 61.10.Ht, 81.07.Nb

I. INTRODUCTION

Among the polycyclic aromatic hydrocarbons considered as active layers for constructing low-cost organic field effect transistors (OFETs), pentacene (Pc, $C_{22}H_{14}$) appears particularly attractive because of its high room temperature charge carrier mobility (1.5 cm^2/V s), which has been reported to match or even surpass that of amorphous silicon.[1]

Pentacene is composed of five benzene rings coupled side by side in a linear planar configuration. In the bulk phase Pc crystallizes in a layered triclinic structure, with the molecules, which are not perpendicular to the lattice planes, assembled into a herringbone arrangement in the (100) plane.[2] The partial overlap between the π orbitals of face-edge interacting adjacent Pc molecules makes possible charge hopping, at the basis of carrier transport in organic crystals, which is then maximal in the direction perpendicular to the long molecular axis. Such anisotropy of the carrier mobility should be exploited in OFET devices, by properly orienting the Pc molecules with respect to the substrate plane, in order to align the preferential hopping direction with the source/drain geometry. Moreover, being carrier transport severely limited by impurities, lattice defects, and grain boundaries, device efficiency can be dramatically enhanced by the choice of suitable substrates, whose chemical and structural properties facilitate Pc heteroepitaxy.

In thin layers, Pc self-assembles into bulklike structures with "standing up" orientation only when the van der Waals (VdW) intermolecular forces are dominant with respect to the interaction with the substrate. Bulklike configurations even at monolayer (ML) thickness, favored by the attenuated surface-adsorbate forces, have been observed in the case of H terminated Si(111),[3] for SiO_2 substrates,[4,5] on well-ordered Bi(001) films,[6] and also on metal substrates functionalized with self-assembled MLs, which break the strong surface/Pc interaction.[7]

On less inert surfaces, the crystallographic orientation of Pc is determined by the balance between the weak VdW-type Pc-Pc interaction and the interaction with the substrate, substantially depending on the electronic structure of the latter. In the case of metal surfaces, the strong interaction between the empty *d* orbitals of the substrate and the π cloud of Pc forces the adsorbed molecules to assume a flat geometry. For coverages up to 1 ML, flat lying Pc has been observed on Cu(111),[8] Cu(100),[9] Cu(110),[10–13] Au(111),[14] Au(100),[15] Fe(100),[16] Ag(110),[17] as well as on the Cu(119) vicinal surface.[18] In general, for coverages above the first ML, the Pc molecules reorient from an initially interface-controlled structure towards a bulklike structure.

Ordering in the first ML is believed to drive the epitaxy in the upper layer, by governing the formation of domains and grain boundaries, which can act as carrier traps. Due to this primary role, the structure of the Pc layer in contact with the substrate has been the subject of several detailed studies. It is found that, mostly, when Pc is deposited at room temperature there is only short range layer ordering and a moderate annealing is necessary to obtain long-range ordered phases.[10] Moreover, for very diluted phases the lack of distinctive diffraction spots in the low energy electron diffraction (LEED) patterns denotes the absence of extended periodic structures.[11] In general, for flat (111) surfaces of weakly interacting metals, steps[18] and anchoring functional groups are indispensable to obtain long range ordering, whereas in the case of (110) templating surfaces, the reduced mobility when approaching ML coverage is sufficient to achieve an ordered layer.[17]

Multiform configurations have been observed on different metal substrates, depending on surface termination, Pc coverage, and annealing temperature. Periodic structures, commensurate with the substrate periodicity, are favoured when the surface lattice spacing matches the distance between ad-

jacent phenyl rings. Several structures might coexist on the same surface.[19–21] Moreover thermal annealing can trigger the transition between different structures in the ML regime[11,21] by inducing layer reorganization or partial desorption.

On several metals Pc deposition beyond the first ML coincides with the transition to a different configuration, which usually corresponds to a rotation of the Pc plane around the long axis which remains parallel to the surface leading to a tilted orientation. The growth of Pc multilayer films was followed in detail on Cu(110).[12,13] Up to 2 nm an intermediate phase, characterized by the molecules tilted around the long axis which remains parallel to the substrate was identified. Above that, a different structure was observed, with the molecules assuming an upright orientation giving a herringbone type arrangement, similar to the Pc bulk structure although with slightly shorter lattice constants. Similar structures have been reported for Pc films grown on quartz or polyester substrates.[22]

Differently from the Pc/Cu (110) (Refs. 10–13) and Pc/Cu(111) (Ref. 8) interfaces, whose adsorption features were well stated by scanning tunneling microscopy (STM), only rarely has the twofold Cu(100) surface been considered as substrate for the growth of Pc or other polyacene layers. Flat lying Pc with a configuration approaching the hexagonal packing was observed by LEED on Cu(100),[9] whereas for tetracene deposited on Cu(100) and Cu(110) Yannoulis *et al.*[23] reported that, already at ML coverage, the long molecular axis was perpendicular to the copper substrate. In comparison with the (110) orientation which is characterized by the absence of rotated domains and by the formation of long-range ordered structures, a weaker tendency towards in-plane ordering is, in principle, expected in the case of the less templating (100) surface.

In this study we have faced the formation of the Pc/Cu(100) interface by using the partial charge method approach to calculate the most probable structures for coverage ranging from sub-ML to multilayer regime. Computations of the energetic parameters are related to the experimental structural information derived from the angular dependent x-ray absorption spectra of a multilayer Pc film on Cu(100).

II. COMPUTATIONAL METHOD

Following the idea of Zerbetto *et al.*[24,25] the total potential energy function V_{TOT} of the system has been approximated by the sum of three terms: the inter- and intra-molecular potential energy of the organic subsystem V_{ORG}, the tight binding potential energy of the metal V_{MET} and the interaction energy between the metallic and organic subsystems $V_{\mathrm{ORG\text{-}MET}}$.

$$V_{\mathrm{TOT}} = V_{\mathrm{ORG}} + V_{\mathrm{MET}} + V_{\mathrm{ORG\text{-}MET}}. \tag{1}$$

The V_{ORG} term is based on the MM3 force field of Allinger *et al.*[26] which is well suited to describe the aliphatic and aromatic hydrocarbons and takes into account electrostatic effects. The second potential term is a tight binding term inclusive of a repulsion intermetallic term

$$V_{\mathrm{MET}} = E_{\mathrm{TB}} = E_{\mathrm{bond}} + E_{\mathrm{TB}}^{\mathrm{rep}}, \tag{2}$$

where E_{bond} is a many body term as obtained by the tight binding second-moment model. The second moment approach of the tight-binding model gives an electronic band energy per atom which has the form of the square root of a pair wise sum of squared hopping integrals $f(r_{ij})$

$$E_{\mathrm{bond}} = -A\sum_i \sqrt{\sum_j f(r_{ij})} = A\sum_i E_i^{\mathrm{BAND}}, \tag{3}$$

where r_{ij} is the distance between the ith and the jth atoms, and A is a constant.

This functional form has been the basis of empirical non-pair wise force models for transition and noble metals. Hitherto, it appeared to be valid for a half-filled band.[27] We have used the expression of the band energy for an atom i as derived by Rosato *et al.*[28]

$$E_i^{\mathrm{BAND}} = -\sqrt{\sum_j \left[\xi_{\alpha\beta}^2 e^{-2q_{\alpha\beta}\left[(r_{ij}/r_0^{\alpha\beta})\right]-1}\right]}, \tag{4}$$

where ξ is an effective hopping integral, $q_{\alpha\beta}$ and $r_0^{\alpha\beta}$ are respectively an empirical parameter depending only on the metallic species α and β and the first-neighbor distance for the studied lattice. The repulsion intermetallic term ($E_{\mathrm{TB}}^{\mathrm{rep}}$), arising from the interaction of the electronic densities localized on the atomic nuclei, is a simple sum of pair wise repulsion terms

$$E_{TB}^{rep} = \sum_{ij} A_{\alpha\beta} e^{-p_{\alpha\beta}\left[(r_{ij}/r_0^{\alpha\beta})\right]-1}, \tag{5}$$

where $p_{\alpha\beta}$ and $A_{\alpha\beta}$ depend on the atomic species α and β and r_{ij} is the distance between atoms i and j. The overall metallic potential is characterized for Cu(100) by the parameters:[26] $A=0.0855$ eV, $\xi=1.224$ eV, $p=10.96$, $r_0=2.556$ Å, and $q=2.278$.

The interaction between the metallic and the organic subsystem ($V_{\mathrm{ORG\text{-}MET}}$) is based on the charge equilibration approach developed originally by Rappe and Goddard[29] plus a short range VdW term (E_{VdW}). The $V_{\mathrm{ORG\text{-}MET}}$ long range term is an electrostatic potential arising from fictional partial charges q_i on the nuclei of the metal atoms and of the organic molecules. The q_i charges are calculated with a formula derived by simple electronegativity equilibration. The total energy of the systems is expressed as a sum of one particle term and of two-body part

$$E = \sum_i E_i + \sum_{i<j} E_{ij}, \tag{6}$$

where E_i is the ith atom electrostatic energy assumed to be differentiable with respect of the atomic partial charge q_i, and E_i^0 is the ith atom electrostatic energy in the case of zero q_i

$$E_i = E_i^0 + q_i\left(\frac{\partial E}{\partial q_i}\right)_0 + \frac{1}{2}q_i^2\left(\frac{\partial^2 E}{\partial q_i^2}\right)_0 + \ldots. \tag{7}$$

Using the Mulliken definition of the atomic electronegativity

$$\chi_i^o = \frac{1}{2}(IP_i + EA_i) = \left(\frac{\partial E}{\partial q_i}\right)_0 \tag{8}$$

and defining the Coulomb repulsion integral between electrons of the same atom (the one-center Coulomb integral)

$$J_{ii} = IP_i - EA_i = \left(\frac{\partial^2 E}{\partial q_i^2}\right)_0 \tag{9}$$

the energy of the ith atom is

$$E_i = E_i^0 + \chi_i^0 q_i + \frac{1}{2} J_{ii} q_i^2. \tag{10}$$

The two-body term is assumed to be a simple two-center Coulomb interactions:

$$E_{ij} = J_{ij} q_i q_j, \tag{11}$$

where the two-center term J_{ij} are calculated by using the semi-empirical equation proposed by Ohno-Klopman[30]

$$J_{ij}(r_{ij}) = \frac{1}{\sqrt{r_{ij}^2 + \left(\frac{1}{2J_{ii}} + \frac{1}{2J_{jj}}\right)^2}}, \tag{12}$$

where r_{ij} is the interatomic distance between the ith and the jth atom. This term depends only on the atomic species and on their distance.

Hence the electronegativity of the ith atom is defined as

$$\chi_i = \frac{\partial E}{\partial q_i} = \chi_i^0 + J_{ii} q_i + \sum_{i \neq j} J_{ij} q_j \tag{13}$$

and according to the principle of electronegativity equalization

$$\chi_1 = \chi_2 = \ldots = \chi_N \tag{14}$$

and to the condition on the total charge of the system

$$Q_{\text{total}} = \sum_i^N Q_i \tag{15}$$

a total of N simultaneous equations are obtained

$$CQ = D, \tag{16}$$

where the vector Q contains all the atomic partial charges of a N atomic systems, and where the C matrix is

$$C_{1j} = 1,$$

$$C_{ij} = J_{1j} - J_{ij} \quad \text{for } i \geqslant 2, \tag{17}$$

and the vector D is

$$D_1 = Q_{\text{total}},$$

$$D_i = \chi_i - \chi_i^0 \quad \text{for } i \geqslant 2. \tag{18}$$

Hence Eqs. (16) are solved at every fixed geometry of the atomic nuclei of the system and given the parameter χ_i and J_{ii} for the different atomic species present in the simulation system. In particular we have used the parameters χ_i and J_{ii} for H, C, and Cu atoms as reported by Thiel *et al.*:[31,32] $\chi_H = 7.17$ eV, $\chi_C = 6.27$ eV, $\chi_{Cu} = 4.48$ eV, $J_{HH} = 12.84$ eV, $J_{C\text{-}C} = 10.00$ eV, and $J_{Cu\text{-}Cu} = 6.50$ eV. The calculated partial charges produce an electrostatic long range potential, which is added to a short range field, that takes into account the nucleus-nucleus repulsion terms and the high order multipole interactions. In particular we have used a Buckingham VdW function

$$E_{vdw}(r) = \varepsilon \left[A e^{-Br/r_0} - C\left(\frac{r_0}{r}\right)^6 \right], \tag{19}$$

where A, B, and C are respectively 184 000.0 $(\text{Kcal/mol})^{-1}$, 12.0 and 2.25 $\text{Kcal/mol}\cdot\text{Å}^6$. The other parameters have been chosen after a tuning procedure: $\varepsilon_{Cu\text{-}C} = 0.039$ Kcal/mol, $\varepsilon_{Cu\text{-}H} = 0.42$ Kcal/mol, $r_0^{Cu\text{-}C} = 2$ Å and $r_0^{Cu\text{-}H} = 3.1$ Å neglecting the attractive part of the E_{VdW} for the Cu-H interaction.

The TINKER program[33] has been modified to take into account the above overall potential energy terms. We have used the periodic boundary conditions (PBC) with orthogonal unit cell and 26 and 8 replica cells for the bulk and surface simulation, respectively. The geometrical optimizations were performed in Cartesian coordinate space using a low storage BFGS nonlinear optimization.[34] The number density (Δ_{Pc}) of Pc molecules has been evaluated as the number of pentacenes in the volume between the metal surface and the topmost point occupied by a Pc atom. The energetic of the multilayers is studied with the help of energy terms:

(I) The Pc cohesive energy

$$E_{\text{Coh}}^{\text{Pc}} = \frac{E_{\text{system}} - E_{\text{metal}} - N_{\text{Pc}} E_{\text{Pc}}^{\text{free}}}{N_{\text{Pc}}}, \tag{20}$$

where E_{system} is the energy of the whole system in the simulation cell, and E_{metal} is the energy of the metal atoms in the absence of the Pc molecules. N_{Pc} is the number of Pc molecules in the cell, and $E_{\text{Pc}}^{\text{free}}$ is the energy of a single free Pc molecule. $E_{\text{coh}}^{\text{Pc}}$ is the average energy needed to remove a Pc molecule from the system formed by the metal copper plus the molecular film.

(II) The reduced molecular cohesive energy evaluated by neglecting the direct interaction of the Pc first layer with the metal

$$\Delta E_{\text{Coh}}^{\text{Pc}} = E_{\text{Coh}}^{\text{Pc}} - \frac{\sum_{\text{all Pc of the first layer}} D_0^{\text{Pc-Cu}}}{N_{\text{Pc}}}, \tag{21}$$

where $D_0^{\text{Pc-Cu}}$ is the binding energy between a single Pc molecule and the solid metal surface. $\Delta E_{\text{coh}}^{\text{Pc}}$ is the average energy to remove a Pc molecule from the molecular film in the hypothesis of neglecting the interaction between the Pc molecules of the first layer and the copper metal. In this way we can monitor the effective forces acting among Pc molecules without the direct interaction of the copper subsystem.

(III) The average energy required to stress the Pc layers from the free film to the absorbed film on Cu metal

$$E_{\mathrm{STRESS}}^{\mathrm{Pc\ film}} = \frac{E_{\mathrm{Pc}}^{\mathrm{film\ on\ Cu}} - E_{\mathrm{Pc}}^{\mathrm{free\ film}}}{N_{\mathrm{Pc}}}. \quad (22)$$

The $E_{\mathrm{STRESS}}^{\mathrm{Pc\ film}}$ energy is a good indicator of the structuring effects of the metal on the absorbed organic molecules. This energy increases when the geometrical structure of the Pc molecules in the film adsorbed on the metal surface is highly distorted with respect to the geometrical structure of the Pc molecules in a free-standing film.

III. EXPERIMENTAL

Pentacene thin films were grown by organic molecular beam epitaxy on a copper substrate. Clean Cu(100) surface was prepared *in situ* according to standard UHV procedures;[35] its atomic cleanliness was checked by near edge x ray absorption fine structure (NEXAFS): no traces of typical contaminants (such as oxygen and sulfur) were detected within the limit of the NEXAFS sensitivity. The substrate was held at room temperature during the organic film deposition. Assuming for the equivalent-monolayer (ML) the bulk density and structure of crystal Pc, a typical growth rate of $\approx$0.5 ML/min, as checked by a quartz microbalance, was obtained by thermally controlling a custom-made Knudsen cell (accuracy better than 0.5 °C).

Angle-dependent NEXAFS experiments were carried out at the BEAR beam line[36] at bending magnet exit 8.1 of the Elettra storage ring (Trieste, Italy). In the present experiment we used a polarization degree better than 80%. Sample holder rotations featured a 10^{-3} deg overall accuracy. We estimate that a major uncertainty (about 1°) on the experimental angle was mostly due to the mechanical mounting of the copper substrate on the holder. A light spot of 30 $\times$300 μm^2 (vertical$\times$horizontal) was used with a resolving power $E/\Delta E \approx 5000$ at the carbon K edge. NEXAFS scans were acquired in the (275–345) eV photon energy range by measuring the sample drain current I_s. Spectra were normalized to the incident photon flux I_0, using the current I_m drained by a tungsten mesh inserted along the beam path, hence measured at the same time as I_s.

We have exploited the well known dependence of the intensity of the optical transitions from the C 1s core level to the first unoccupied electronic states, as a function of the angle between the electric field polarization vector **E** and the direction of maximum orbital amplitude. This method is quite general and nowadays well established and based on the fact that the absorption intensity is proportional to $|\mathbf{E}\cdot\mathbf{T}|^2$, where **T** is the transition dipole moment of the selected orbitals.[37] Polarization-dependent NEXAFS spectra have been measured by varying the angle between the polarization **E** vector of the incident beam and the normal $\hat{\mathbf{n}}$ to the copper surface. The angle scan was achieved by rotating the polar angle α of the sample with respect to the incident photon beam direction (**k**).

After applying the procedure for I_0 correction, all spectra have been brought to the same scale by normalizing them to the atomic edge jump, namely by bringing to the same level the intensities for photon energy well below the C K edge and for photon energies well above the near-edge structures.

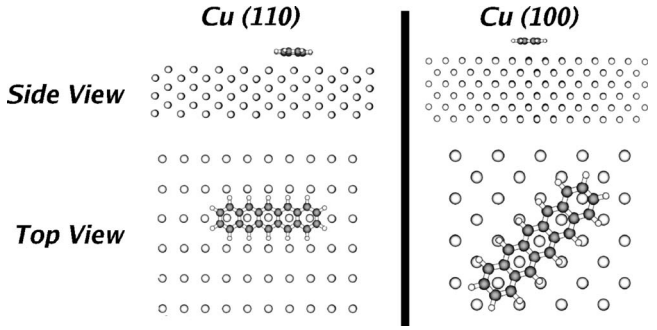

FIG. 1. Side and top views of a single pentacene molecule adsorbed on the Cu(110) and Cu(100) surfaces.

IV. RESULTS

A. Single pentacene molecule on Cu surfaces

We have simulated as a test case the bulk Cu in an orthogonal unit cell of $25.27\times25.27\times11.00$ Å^3 with a total of 15 876 atoms including the replica of the PBC. The cohesive energy has been calculated to be 3.52 eV, in good agreement with experimental finding of 3.54 eV.[38] The metal surface system has been calculated for the two (100) and (110) faces: the dimensions of the unit cells were the above ones for the (100) face and $25.52\times32.49\times15.00$ Å^3 for the (110) face, and the replica for the PBC is up to nine unit cells. Their atomic cohesive energies have been calculated as 3.364 eV (100) and 3.266 eV (110).

The case of a single Pc molecule absorbed on the Cu surface has been analyzed with respect to the (110) and (100) faces. On both Cu(100) and Cu(110) surfaces the Pc molecule lies with the aromatic rings parallel to the metal surface at a distance of 2.5 Å (Fig. 1) and has a binding energy $D_0^{\mathrm{Pc\text{-}Cu}}$ of 2.2 eV. This value is in good agreement with the experimental value of about 2.2 eV measured for monolayer Pc molecules absorbed on Cu(110) (Ref. 12). In both cases the center of the Pc molecules resides at the Cu top site, whereas the lateral aromatic rings are slightly misaligned with the respect to the underlying Cu atoms, due to the slight mismatch between the Cu-Cu distance (2.55 Å) and the distance between adjacent aromatic rings (2.39 Å) in Pc.

In Fig. 2 we report the partial charge distribution on the Cu(100) surface induced by the presence of a Pc molecule.

B. Pentacene monolayer on Cu(100)

The monolayer coverage of the (100) Cu surface has been studied with regard to the different topologies the system can

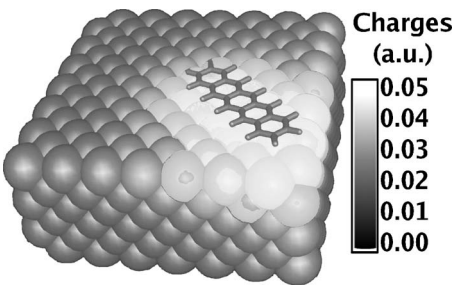

FIG. 2. Partial charge distribution in a.u. (atomic units, i.e., one electron charge) on the Cu(100) lattice ions induced by the adsorption of a single pentacene molecule.

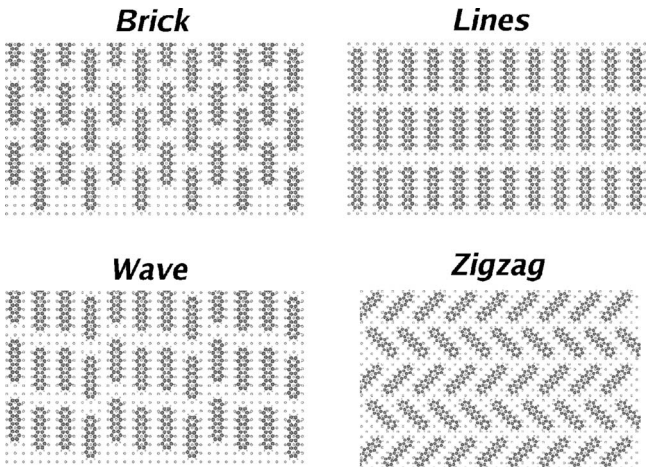

FIG. 3. Geometry configurations of four different topologies calculated for the pentacene monolayer adsorbed on Cu(100).

sustain. In particular we have found that the Pc molecules adsorbed on the Cu(100) surface at saturation coverage originate four characteristic topologies which we have named as Brick, Lines, Wave, and Zigzag shown in Fig. 3 and described hereafter, whereas the corresponding energetic parameters are listed in Table I. In each case the Pc molecules lie with the aromatic rings parallel to the metal surface.

The Brick configuration is represented in Fig. 3 and is characterized by staggered rows of Pc lying above the Cu surface at about 3 Å. Each row is centered 7.7 Å apart from the next ones. Every Pc has six H atoms fronting (2.5 Å apart) other six hydrogens of Pc molecules of the neighbor rows, and every Pc has four hydrogens facing at about 4.5 Å four H atoms of the two adjacent Pc molecules in the same molecular row.

The Lines topology is formed by regular Pc rows, about 7.7 Å far from each other, lying parallel to the metal surface at a distance of 2.9 Å. Every H fronts a corresponding H of a neighbor Pc, at a distance of about 2.5 Å as can be seen from Fig. 3. This configuration has the highest $E_{\mathrm{coh}}^{\mathrm{Pc}}$ energy (3.48 eV) with respect to the other monolayer geometries.

The third monolayer configuration is the Wave one: here the rows of Pc are similar to the Lines geometry, but they are partially staggered so that not all the H atoms face directly other hydrogens. The rows of Pc are planar with respect to the metal surface at a distance of 2.95 Å.

The Zigzag geometry is a compact topology (2.51 Pc for each nm^3) 2.9 Å far from the Cu (100) face. Likewise the Wave case the direct facing of H atoms is partial and at a distance of about 2.5 Å.

C. Pentacene multilayers on Cu(100)

The multilayers structural search was based on BFGS (Broyden, Fletcher, Goldfarb, and Shanno) quasi-Newton optimization[39] of random chosen initial multilayer configurations, and the rms gradient per atom was fixed at 0.01 Kcal/mol/Å as the stability criterion. Pentacene multilayers are supported only by the Brick and Wave topologies. A particular case is represented by the Lines geometry, on which it seems only a bilayer structure is stable, and multi-

TABLE I. Energetic parameters as a function of the pentacene layer number, topology, and Pc number density Δ_{Pc}. The reported parameters are: the cohesive energy $E_{\mathrm{coh}}^{\mathrm{Pc}}$, the reduced molecular cohesive energy $\Delta E_{\mathrm{coh}}^{\mathrm{Pc}}$, the average energy required to stress the Pc layers from the free film to the film adsorbed on Cu metal $E_{\mathrm{STRESS}}^{\mathrm{MET}}$, the total charge dipole energy $E_{q-\mu}^{\mathrm{TOT}}$, the dipole-dipole energy per Pc molecule $E_{\mu-\mu}^{\mathrm{Pc}}$, and the torsional energy of the Pc molecules $E_{\mathrm{tors}}^{\mathrm{Pc}}$.

Number of layers	Topology	Δ_{Pc} (nm^{-3})	$E_{\mathrm{coh}}^{\mathrm{Pc}}$ (eV)	$\Delta E_{\mathrm{coh}}^{\mathrm{Pc}}$ (eV)	$E_{\mathrm{STRESS}}^{\mathrm{MET}}$ (eV)	$E_{q-\mu}^{\mathrm{TOT}}$ (eV)	$E_{\mu-\mu}^{\mathrm{Pc}}$ (eV)	$E_{\mathrm{tors}}^{\mathrm{Pc}}$ (eV)
1	Brick	2.39	3.19	1.0	0.5	−0.22	0.39	−1.04
	Line	2.52	3.48	1.28	0.5	−0.26	0.39	−1.02
	Wave	2.47	3.37	1.16	0.6	−0.30	0.39	−1.03
	Zigzag	2.51	3.42	1.24	0.5	−0.39	0.39	−1.03
2	Brick LD	1.36	1.77	0.36	0.4	0.09	0.35	−1.06
	Line	2.30	1.88	1.08	0.5	0.69	0.40	−1.05
	Wave	1.95	1.63	0.77	0.5	0.30	0.41	−1.06
3	Brick LD	1.67	1.35	0.44	0.5	0.13	0.35	−1.06
	Brick HD	2.32	1.73	1.24	0.5	−0.48	0.36	−1.06
4	Brick HD	2.42	1.62	1.23	0.5	−0.43	0.34	−1.06
5	Brick LD	1.54	1.01	0.46	0.5	0.09	//	−1.07
	Brick HD	2.13	1.51	1.18	0.5	−0.43	0.36	−1.06
	Wave	2.10	1.49	1.02	0.4	0.26	0.33	−1.07
6	Brick LD	1.44	0.98	0.54	0.4	−0.04	0.33	−1.07
	Brick HD	2.03	1.45	1.17	0.5	−0.39	0.34	−1.07
7	Wave	2.18	1.43	1.11	0.4	0.35	0.31	−1.07
9	Wave	2.27	1.42	1.18	0.4	0.48	0.29	−1.07

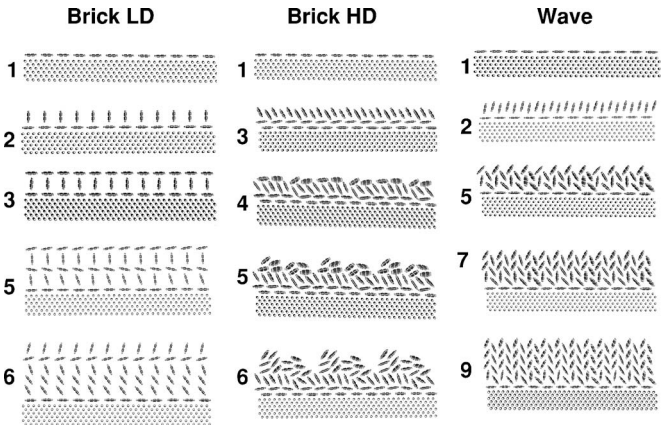

FIG. 4. Low density Brick, high density Brick and Wave topologies with different number of pentacene layers.

layers seem not to withstand stress without structural damage or distortion.

In the following we report the structural and energetic information up to the ninth layer for the Wave geometry, and up to the seventh layer for the Brick geometry; for the latter, stable multilayer structures can be classified in two types according to their low or high density of Pc molecules. The different structures are illustrated in Fig. 4.

The low density (LD) Brick multilayers are reported for 2, 3, 5, and 6 layers. The second layer is perpendicular to the first one with the long molecular axis always parallel to the metal surface. This is not a very compact structure, and has a Pc number density of 1.36 mol/nm^3. The third layer has the same geometry as the first one, but is shifted of 10.3 Å away from the Cu surface. In the 5-layer structure molecules of the second and fourth layers have the short axes tilted by 60°–90°, whereas the third and fifth layers are almost equal to the first one. In the 6–layer system the quasiordered geometry of the thinner multilayers seems a bit more unstructured: here the second, third, fourth, and sixth layers have the short axes tilted in a random way.

The high density (HD) Brick multilayers have been studied for 3, 4, 5, and 6 layers. In particular the 3-layer structure is characterized by the second layer with a topology similar to the first layer, but laterally shifted as to have its H atoms facing the C atoms of the first layer. In the third layer the Pc molecules have their short axes tilted by about 60° with respect to the Cu face. The 4-layer system is similar to the 3-layer one, plus a layer of Pc molecules almost parallel to the copper surface. In the 5-layer and 6-layer HD Brick structures, the first three layers keep the configuration observed in thinner multilayers, whereas the outermost layers reveal irregular and disordered orientations, and exhibit a sort of island structures.

The Wave multilayer topologies have been studied for 1, 2, 5, 7, and 9 layers (Fig. 4). In all these multilayer systems the Pc molecules have a herringbonelike structure but in the bilayer, where the Pc molecules are lined up in a regular way. The Wave multilayers are the bulk-Pc most resembling ones, and have a herringbone structure and an intermolecular energy of 1.30 eV per each Pc.[40]

The structural information relative to all the above topologies, studied at different multilayers coverage, can be analyzed with regard to their energetic properties. In Table I we have given an account of some detailed energetic parameters as a function of topology, numbers of layers, and number density. In particular the energy analysis has been related to two structural parameters: the Pc number density (Δ_{Pc}) and the Pc film thickness.

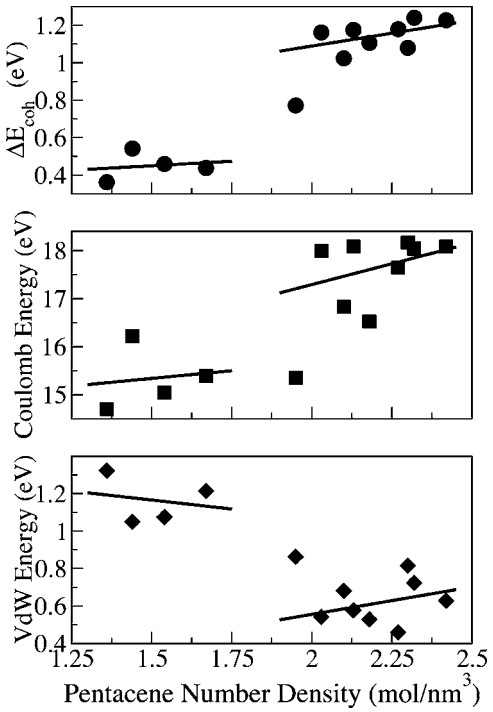

FIG. 5. Dependence of the energetic parameters on the Pc number density.

In Fig. 5 we report ΔE_{coh}^{Pc}, the Coulomb energy due to the electrostatic interaction among partial charges, and the VdW intermolecular energy as a function of the Pc number density. Although there is no clear dependence of these energies on Δ_{Pc}, it appears evident that the compact topologies are characterized by a higher intermolecular energy content, and that this is mainly due to an increase of the attractive Coulomb energy and to a decrease of the VdW inter-Pc energy.

Figure 6 reports the $E_{STRESS}^{Pc\ film}$ energy as a function of the Pc film thickness. Data are grouped in two sets: the low density phase, with Δ_{Pc} values in the range 1.4–1.7 mol/nm^3, and the high density phase with Δ_{Pc} between 2.0–2.4 mol/nm^3.

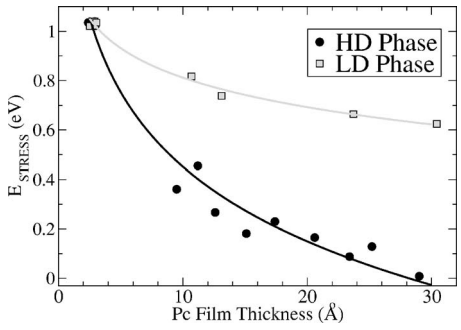

FIG. 6. Stress energy vs thickness for low density and high density pentacene films deposited on Cu(100).

The latter has an almost vanishing $E_{\mathrm{STRESS}}^{\mathrm{Pc\ film}}$ at Pc film thickness of about 30 Å, whereas the corresponding values for the low density phase are still about 0.6 eV. The influence and templating effect of the Cu surface on the Pc film growth decreases faster for the high density than for the low density phase. Table I reports $E_{\mathrm{STRESS}}^{\mathrm{MET}}$ for the different Pc structures. This is the energy required to change the geometry of the metal system from the bare state to the actual Pc multilayer state: this energy is connected with the deformation of the metal ion lattice due to the interaction with the Pc molecules. The data listed in Table I show that $E_{\mathrm{STRESS}}^{\mathrm{MET}}$ does not depend on Δ_{Pc}, and it is of the order of 0.5 eV for all the multilayers simulated in the cell here considered. This reflects the weak energetic effects produced by the Pc film on the Cu metal in agreement with the localized substrate perturbation deduced by studying the partial charges localization in the case of a single Pc molecule absorption (see Fig. 2). A similar weak dependence on Δ_{Pc} is observed for the dipole-dipole interaction energies ($E_{\mu\text{-}\mu}^{\mathrm{Pc}}$) and the torsional deformation energies ($E_{\mathrm{tors}}^{\mathrm{Pc}}$). These interactions are weakly dependent on both the size and the topology of the systems. On the contrary the Pc cohesive energy ($E_{\mathrm{coh}}^{\mathrm{Pc}}$) and the charge-dipole interactions ($E_{q\text{-}\mu}^{\mathrm{TOT}}$) are strongly dependent on the specific topology and Pc density, although it seems there is not a clear trend in these energetic parameters. In particular the $E_{q\text{-}\mu}^{\mathrm{TOT}}$ values are strongly scattered with respect to the geometrical parameters. These types of energy do not characterize the Pc films. At this regard $\Delta E_{\mathrm{coh}}^{\mathrm{Pc}}$, the Coulomb and the VdW energies, reported in Fig. 5 as a function of Δ_{Pc}, reveal that the low and high density phases are characterized by well defined different energetic contents. In the low density phase the Pc molecules interact among themselves weakly with respect to the Pc molecules of the high density phase. In particular in the low density phase the attractive Coulomb energy is smaller and the repulsive VdW energy is larger in comparison to the high density phase. This suggests that the Pc molecules of the low density phase are more strongly influenced by the copper surface in term of templating effects: their lower reduced cohesive energies $\Delta E_{\mathrm{coh}}^{\mathrm{Pc}}$ are connected with higher interactions among Pc molecules and Cu atoms.

D. NEXAFS Spectroscopy of a pentacene multilayer on Cu(100)

In Fig. 7 are shown NEXAFS spectra measured at different polar angles (α) on a pentacene film of 4 MLs as-deposited on the Cu (001) surface. A sketch of the experiment geometry is shown in the inset of Fig. 7 (**k**, **E**, and $\check{\mathbf{n}}$ are coplanar). The molecular tilt angle γ formed by the normal $\hat{\mathbf{c}}$ to the aromatic rings with respect to the copper surface normal $\check{\mathbf{n}}$ is also displayed.

The gross features in absorption spectra can be explained in terms of transitions from the C 1*s* core level towards the lowest unoccupied molecular orbitals, though the resonances in the near-edge region are characterized by core-hole final state effects with possible excitonic contribution that are typical of poly-conjugated π-electron systems.[41] Two main manifolds characterize the near-edge signal, in the 284–290 eV photon energy range, most of them ascribable to $1s\text{-}\pi^*$ resonances of the Pc molecule, whereas the four

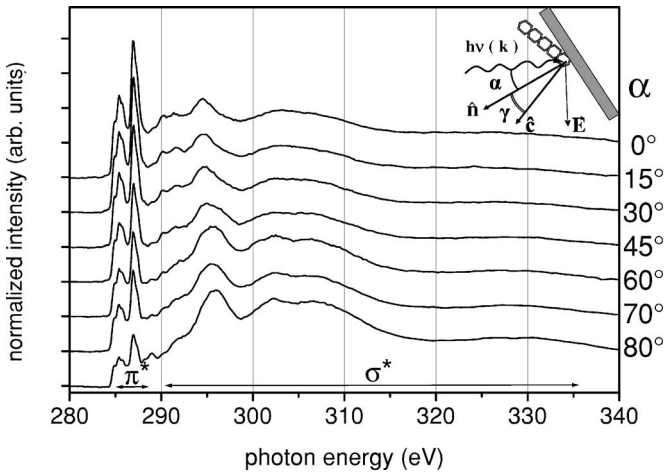

FIG. 7. NEXAFS spectra measured at different polar angles α for a 4 ML Pc film deposited on Cu (001). A sketch of the experiment geometry is shown in the insert (the incident photon beam direction **k**, the polarization **E** and the normal $\check{\mathbf{n}}$ to the substrate are coplanar). The molecular tilt angle γ formed by the normal $\hat{\mathbf{c}}$ to the aromatic rings with respect to $\check{\mathbf{n}}$ is also displayed.

broad features visible at higher energy, extending up to 340 eV, are ascribable to σ^* empty states. Both π manifolds compare well with the energy positions of the correspondent gas-phase measurements.[42] The similitude in absorption line shapes of the Pc film and the free Pc molecule reflects the absence of significant variation of the unoccupied electronic states, this being an indication of weak intermolecular forces.

Our NEXAFS data show a strong variation with the polar angle α, that is explained in terms of polarization-dependent transitions according to the dipole selection rules for linearly polarized photons: in planar aromatic systems when **E** vector is parallel to the $\hat{\mathbf{c}}$ axis (normal to the molecular plane), $\mathbf{E}_{\parallel}\hat{\mathbf{c}}$, only transitions changing the parity sign ($1s \rightarrow \pi^*$) are allowed, while, for $\mathbf{E} \perp \hat{\mathbf{c}}$, only $1s \rightarrow \sigma^*$ transitions are allowed. The spectral features show strong angle dependence: for increasing α the intensities of the π^* state contributions are reduced, while the σ^* ones increase.

According to the literature, all the spectral features up to 290 eV are considered to have π character; nonetheless the angle dependence of the intensities at 287.3 eV and 288.8 eV in our data could suggest a contribution from empty states with different symmetry, in particular of σ character for latter feature. The pronounced dichroism of both the π^* and the σ^* resonance intensities indicates a high degree of molecular orientation in which the aromatic rings are tilted by the angle γ. This structural information has already been achieved by polarization-dependent NEXAFS studies of Pc growth on Cu(110) (Ref. 12) and on both insulating[4] and other noble metal substrates.[14]

In order to highlight our interpretation of the experimental findings, difference-spectra are reported in Fig. 8 obtained by subtracting the absorption intensity at $\alpha=0°$ from the ones measured for different values of α. Although possible saturation effects[43] are not taken into account in this analysis, this way of handling the data helps to better follow the trend of the measurements as a function of the polar angle α. The spectral features depending on the orientation are enhanced,

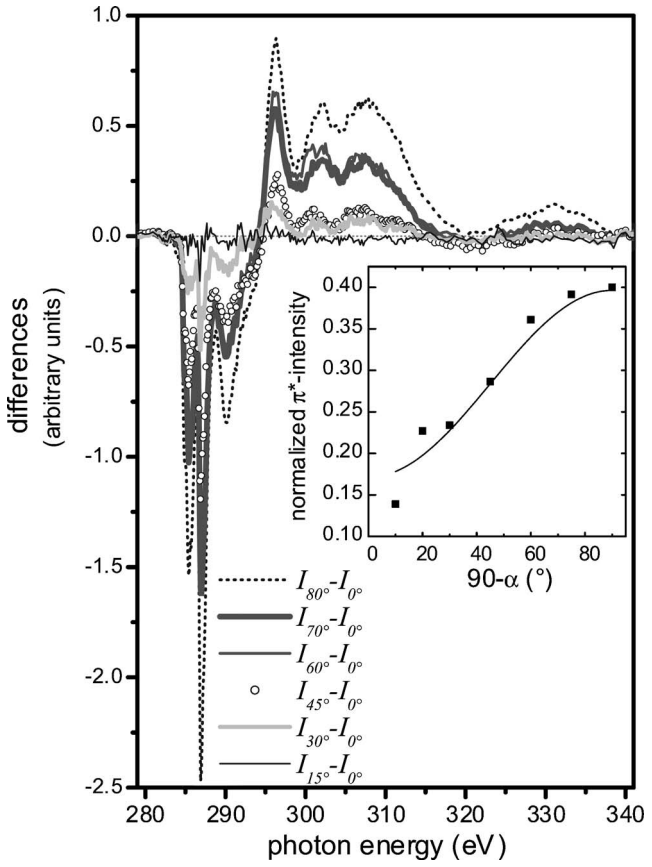

FIG. 8. Difference spectra obtained by subtracting the absorption intensity measured at polar angle $\alpha=0°$ from the ones measured for different values of α. In the insert the angle dependence of the π^* manifold intensity is displayed together with the fitting function (Ref. 37) used to derive the average tilt angle $\gamma=65°$ of the Pc molecules with respect to the copper substrate.

and all the components related to the randomly oriented part of the film, which should provide an isotropic contribution, are neglected. From the quantitative analysis of both difference spectra and angle-dependence of the π^*-resonance intensities,[21] an average value of the tilt angle $\gamma=65°\pm15°$ can be inferred from our experiment (see insert of Fig. 8). However it cannot be established with this set of data whether such a tilt angle is achieved by tilting the molecule around the long axis or by an upright orientation of the molecules.

For what concerns the estimation of the tilt angle γ, two considerations are worth noticing: (i) the sampling depth of the total electron yield is comparable with the nominal thickness of the film; (ii) island formation cannot be excluded on the basis of both resonant photoemission spectra measured on the same system,[44] in which a significant contribution from the copper substrate is visible, and of an atomic force microscopy study of Pc multilayer growth on Au(111) at room temperature.[14] For both reasons a significant contribution from the first Pc layer in contact with the surface, expected to lie flat on the substrate, could give rise to a broadening of the angle dependence of the measured absorption intensity and to an underestimation of the tilt angle. Nonetheless it is worth noticing that the average angle derived by the analysis of the NEXAFS data for our film falls in the range of values measured with same technique for Pc-multilayers of comparable thickness grown on noble metal surfaces.[12–14]

V. DISCUSSION

The calculation reported in Fig. 1 shows that a single Pc molecule adsorbed on Cu(110) and on Cu(100) adopts a lying down configuration, resulting from the strong interaction between Pc and the metal surface. It can be seen from Fig. 2 that the partial charges on the Cu atoms under the aromatic rings are of the order of 0.045 a.u. and that their neighboring Cu atoms have a partial charge around 0.015 a.u This reflects the short range perturbation of the Cu metal by the Pc molecules: only the first two topmost Cu layers are involved in the interaction with the organic molecule. Similar planar configurations, where the substrate-Pc interaction overcomes the Pc-Pc forces leading to molecules lying flat, have been observed for monolayer Pc adsorbed on several metals, regardless of their surface symmetry, such as Cu(011),[10–13] Cu(111),[8] Cu(100),[9] Cu(119),[18] Fe(001),[16] Au(001),[15] Au(111),[14] Ag(111) (Ref. 45) and calculated for Au(001),[46] and Al(001),[47] and Ag(110).[17] The calculated Pc-Cu distance are between 2.9 and 3 Å, which are larger than the effective layer thickness of 1.9 (±0.2) Å measured by helium atom scattering for Pc adsorbed on Cu(110).[12]

Figure 1 shows that Pc molecules lie with the long axis parallel to the [001] lines on Cu(001) and to [110] lines on Cu(110) and with the central aromatic ring centered at the Cu top site. The close matching between the distance of aromatic neighboring ring centers (2.39 Å) and the Cu-Cu atomic distance (2.55 Å) determines a displacement of only 0.32 Å between the center of the terminal phenyl units and the underlying Cu atoms, allowing the formation of commensurate superstructures. Top site adsorption with the long Pc axis aligned with the [110] direction has been proposed to explain the $c(12\times2)$ and $p(6\times22)$ periodicity observed by LEED at saturation coverage of Pc on Cu(110).[11] On the contrary for metal substrates with less favorable lattice matching, adsorption of the Pc center at bridge sites with the molecular longitudinal axis aligned to the [110] direction or rotated with respect to the [001] direction have been calculated for Au(001) (Ref. 45) and Ag(110),[17] respectively.

All four configurations (Brick, Wave, Lines, and Zigzag) calculated for the Pc/Cu(100) interface saturate at surface density of 7.3×10^{13} mol/cm^2. It is worth comparing this number with the maximal surface density of 4×10^{13} mol/cm^2 found for Pc/Cu(110) interface, above which the formation of a multilayer was observed to start.[10]

The Lines morphology resembles the one dimensional rows observed on Au(111),[19,20] on Au(100),[15] and on Cu(011) (Ref. 10) formed by Pc molecules aligned side-by-side perpendicular to the row direction. In the latter case,[10] adjacent molecules are separated by 7.2 Å and form stripes running along the [001] direction with an average inter-row distance of 26–30 Å. In comparison, Pc molecules arranged in the Lines structure adopt a higher packing density having a similar separation of 7.65 Å between the two adjacent mo-

lecular axis, but a lower inter-row separation of 17.85 Å. Even more packed Lines structures were observed by STM for Pc adsorbed on Au(100), the molecular structure being described by unit cells sized with the molecular VdW dimensions.[15]

In both Brick and Wave cases molecular staggering diminishes the H-H repulsion by allowing some H atoms not to face the H atoms of the neighboring molecules. A slight similarity can be found between the Wave topology and the periodic wavelike structures observed by STM on the Pc/Cu(110) surface.[11] In the latter case, however, the waving conformation originated from the periodic staggering inside the Pc rows, where each molecule was shifted by half of the Cu-Cu lattice constant and the resulting alternate top and bridge configurations led to CH interdigitation.[11]

Evolution beyond the first layer depends on the balance between the templating effect of the monolayer and the minimum energy configuration of the pure Pc crystal. Among Brick, Wave, Zigzag and Lines structures which yield, in order, cohesive energies ($E_{\mathrm{coh}}^{\mathrm{Pc}}$) increasing from 3.19 to 3.48 eV, we have found only the first two configurations able to sustain stable multilayer structure. It has to be noticed that in our calculations the thermodynamic effects are neglected, and that all the results are associated with a temperature of zero Kelvin. For Brick HD multilayer assembling coincides with the onset of disorder, whereas in the case of Brick LD and Wave, ordered structures form up to the growth of six and nine layers, respectively. In both cases however, molecules in the second layer assemble with the short molecular axis tilted with respect to the surface plane, still keeping the long molecular axis parallel to the substrate. A similar geometry was observed by Pc molecules deposited on Cu(110) (Refs. 12 and 13) and Ag(111) (Ref. 45) surfaces, where the first flat monolayer is covered by molecules tilted around the long axis which remains parallel to the substrate. A comparison with the Au(100) that has the same twofold symmetry as our substrate also suggests a change in molecular orientation occurring at approximately 3 ML coverage.[15] We find that the thickness of the second layer, with respect to the first, is 1.8 and 1.5 Å respectively for Brick LD and for Wave, which is in agreement with the value of 1.8 (±0.4)*Å* found for the weakly bounded second layer Pc on Cu(110).[12]

In the Wave structure, Pc molecules assemble beyond the second layer maintaining an average tilt angle of 20-25° between the short molecular axis and the surface. The resulting structure closely resembles the herringbone ordering of a bulk Pc crystal oriented with the *b-c* planes parallel to the substrate, proposed for Pc molecules deposited on Ag(111) at coverage above 1 ML.[45] A similar rotated herringbone configuration, with the short axis of the Pc molecules forming an angle of 28° with the surface and the *a-b* plane of the Pc crystal perpendicular to the actual growth plane was observed for thin Pc multilayers deposited on Cu(110).[12,13] This structure was identified as a transition phase between the flat monolayer and the bulklike Pc structure observed at higher layer thickness, with the *a-b* planes of the Pc crystal, parallel to the Cu surface, formed by layers of standing up molecules.[48] The Wave structure calculated in Fig. 4 shows that the rotated herringbone structure maintains up to nine layers (whole thickness of 2.9 nm) at $T=0$ K, whereas for the Pc/Cu(110) system[12,13] deposited at 300–350 K, the interplay of adsorption energy, stress and surface energy sets the phase transition to the upright molecular orientation for layer thickness exceeding 2 nm. This film orientation has not been found by our calculation as the most stable configuration for few layers coverage, even if it could be an higher energy minimum of the total potential energy, and hence populated at room temperature.

Different considerations can be formulated to comment the evolution of the Brick LD structure. Our calculations show the assembling of a second layer of molecules with the long axis parallel and the short axis tilted of 90° with respect to the surface, which are surmounted by a third layer of molecules oriented nearly parallel to the substrate. Even in this case the face to edge molecular orientation bears a resemblance to the parallel-tilted-parallel herringbone structure. It is interesting to note that a similar structure was proposed by France *et al.*[20] who followed by STM the growth of Pc on Au(111) and observed wide spaced rows of tilted molecules, lying above the flat molecules of the first layer and, above them, Pc molecules arranged in a face to face configuration resembling the first layer ordering.

For the Cu(100) surface there is a lack of detailed studies aimed at following the Pc growth on the Cu(100) surface. The few available data reported for the tetracene on Cu(100) reveal a standing up molecular orientation for films only 1-2 ML thick.[23] Such data interpretation was recently confuted by Chen *et al.*[11] who argued that the tetracene layer thickness was underestimated and linked the reported results to much thicker layers. If this is the case, due to the similarity between tetracene and Pc, also in the latter case standing up molecules should characterize the multilayer film grown on Cu(100), in agreement with what has been observed for thick Pc layers on Cu(110) (Refs. 12 and 13) and Au(111),[14] as well as on several inert substrate surfaces.[3–6]

Such growth modality is also sustained by thermodynamic considerations, which find that the (100) surface of Pc crystals is the less energetic and that the intralayer Pc-Pc interaction is stronger than the interlayer interaction, thus favoring the growth of a Pc crystals with the (100) plane parallel to the substrate.[40]

To this conclusion points also our NEXAFS analysis of the 4 ML Pc film grown at room temperature on Cu(100) reported in Figs. 7 and 8. The evident dichroism exhibited by the spectra measured at different angles testifies the presence of a predominant orientation of the empty π^* orbitals with respect the substrate plane, which allows us to exclude a growth type described by the Brick HD model. On the basis of the NEXAFS data it is not possible to state weather the Pc molecules lie with the long or the short molecular axis parallel to the substrate surface. However the fact that the deduced average tilt angle of 65° between the molecular and the surface planes closely resembles the values of 62° and 73° found for several nm Pc films grown on Au(111) (Ref. 14) and Cu(110),[12,13] respectively, both configuration arising from standing-up molecules, suggests also for the multilayer film grown on Cu(100) a similar upright orientation of the Pc molecules.

VI. CONCLUSIONS

By using the partial charge method tight binding approach we calculated the most probable structures for the Pc/Cu(100) interface, for coverages between sub ML and multilayers. Isolated Pc molecules adsorb on Cu surfaces inducing only a short range perturbation of the metal, which is limited to the two topmost lattice atomic layer. For the ML coverage at saturation four stable configurations were calculated, all of them made up by lying down Pc molecules, arranged in a side-by-side fashion with the phenyl rings centered over the top sites. In most of the cases adsorption beyond the first ML is characterized by the molecular plane tilted around the long molecular axis. Subsequent layers tend mainly to assemble in a parallel-tilted-parallel geometry which tends to replicate the typical herringbone geometry of the Pc bulk crystal. The presence of a dominant molecular ordering in the multilayer film deposited on Cu(100) is also indicated by the strong dichroism observed in the NEXAFS spectra.

Calculations predict at $T=0$ K the formation of low density multilayers, where the prevailing templating effect of the substrate counteracts the self assembling of ordered layers, and high density multilayers, that, due to the stronger intramolecular interactions, rapidly converge towards the bulk-like structure. Further experimental work could demonstrate the possibility of switching between the two density regimes, by properly choosing the deposition conditions responsible to determine the structural properties of the organic film.

ACKNOWLEDGMENTS

We are indebted with the staff of the BEAR-beam line at Elettra storage ring (Trieste-Italy) for technical support; in particular we are grateful to N. Mahne for invaluable assistance.

[1] C. D. Dimitrakopoulos, J. Kymissis, S. Purushothaman, D. A. Neumayer, P. R. Duncombe, and R. B. Laibowitz, Adv. Mater. (Weinheim, Ger.) **11**, 1372 (1999).
[2] C. C. Mattheus, G. A. de Wijs, R. A. de Groot, and T. T. M. Palstra, J. Am. Chem. Soc. **125**, 6323 (2003).
[3] T. Shimada, H. Nogawa, T. Hasegawa, K. Ueno, and K. Saiki, Appl. Phys. Lett. **87**, 061917 (2005).
[4] T. Schwieger, X. Liu, D. Olligs, M. Knupfer, and Th. Schmidt, J. Appl. Phys. **96**, 5596 (2004).
[5] S. E. Fritz, S. M. Martin, C. D. Frisbie, M. D. Ward, and M. F. Toney, J. Am. Chem. Soc. **126**, 4084 (2004).
[6] J. T. Sadowski, T. Nagao, S. Yaginuma, Y. Fujikawa, A. Al-Mahboob, K. Nakajima, T. Sakurai, G. E. Thayer and R. M. Tromp, Appl. Phys. Lett. **86**, 073109 (2005).
[7] W. S. Hu, Y. T. Tao, Y. J. Hsu, D. H. Wei, and Y. S. Wu, Langmuir **21**, 2260 (2005).
[8] J. Lagoute, K. Kanisawa, and S. Fölsch, Phys. Rev. B **70**, 245415 (2004).
[9] T. J. Schuerlein, A. Schmidt, P. A. Lee, K. W. Nebesny, and N. R. Armstrong, Jpn. J. Appl. Phys., Part 1 **34**, 3837 (1995).
[10] S. Lukas, G. Witte, and C. Wöll, Phys. Rev. Lett. **88**, 028301 (2002).
[11] Q. Chen, A. J. McDowall, and N. V. Richardson, Langmuir **19**, 10164 (2003).
[12] S. Söhnchen, S. Lukas, and G. Witte, J. Chem. Phys. **121**, 525 (2004).
[13] S. Lukas, S. Söhnchen, G. Witte and C. Wöll, ChemPhysChem **5**, 266 (2004).
[14] G. Beernink, T. Strunskus, G. Witte, and Ch. Wöll, Appl. Phys. Lett. **85**, 398 (2004).
[15] O. McDonald, A. A. Cafolla, D. Carty, G. Sheerin, and G. Hughes, Surf. Sci. **600**, 3217 (2006).
[16] T. Suzuki, M. Kurahashi, X. Ju, and Y. Yamauchi, Surf. Sci. **549**, 97 (2004).
[17] Y. L. Wang, W. Ji, D. X. Shi, S. X. Du, C. Seidel, Y. G. Ma, H.-J. Gao, L. F. Chi, and H. Fuchs, Phys. Rev. B **69**, 075408 (2004).
[18] L. Gavioli, M. Fanetti, M. Sancrotti, and M. G. Betti, Phys. Rev. B **72**, 035458 (2005).
[19] P. G. Schroeder, C. B. France, J. B. Park, and B. A. Parkinson, J. Appl. Phys. **91**, 3010 (2002).
[20] C. B. France, P. G. Schroeder, J. C. Forsythe, and A. Parkinson, Langmuir **19**, 1274 (2003).
[21] J.-Z. Wang, K.-H. Wu, W.-S. Yang, X.-J. Wang, J. T. Sadowski, Y. Fujikawa, and T. Sakurai, Surf. Sci. **579**, 80 (2005).
[22] T. Minakata, H. Imai, M. Ozaki, and K. Saco, J. Appl. Phys. **72**, 5220 (1992).
[23] P. Yannoulis, R. Dudde, K. H. Frank, and E. E. Koch, Surf. Sci. **189/190**, 519 (1987).
[24] R. J. Baxter, G. Teobaldi, and F. Zerbetto, Langmuir **19**, 7335 (2003).
[25] S. Rapino and F. Zerbetto, Langmuir **19**, 2512 (2003).
[26] N. L. Allinger, Y. H. Yuh, and J.-H. Lii, J. Am. Chem. Soc. **111**, 8551 (1989).
[27] M. W. Finnis and J. E. Sinclair, Philos. Mag. A **50**, 45 (1984).
[28] F. Cleri and V. Rosato, Phys. Rev. B **48**, 22 (1993).
[29] A. K. Rappe″ and W. A. Goddard III, J. Phys. Chem. **95**, 3358 (1991).
[30] A. Oda and S. Hirono, J. Mol. Struct. **634**, 159 (2003).
[31] D. Bakowies and W. Thiel, J. Comput. Chem. **17**, 87 (1996).
[32] R. G. Parr and R. G. Pearson, J. Am. Chem. Soc. **105**, 7512 (1983).
[33] P. Ren and J. W. Ponder, J. Phys. Chem. B **107**, 5933 (2003); P. Ren and J. W. Ponder, J. Comput. Chem. **23**, 1497 (2002).
[34] R. H. Byrd, P. Lu, and J. Nocedal, C. Y. Zhu, SIAM J. Sci. Comput. (USA) **16**, 1190 (1995).
[35] G. Musket, W. Mc Lean, C. A. Colmenares, D. Makowiecki, and W. J. Siekhaus, Appl. Surf. Sci. **10**, 143 (1982).
[36] G. Naletto, M. G. Pelizzo, G. Tondello, A. Giglia, and S. Nannarone, Proc. SPIE **4145**, 105 (2001).
[37] J. Stöhr, *NEXAFS Spectroscopy* (Springer, New York, 1996), Vol. 25; J. Stöhr, K. Baberschke, R. Jaeger, R. Treichler, and S. Brennan, Phys. Rev. Lett. **47**, 381 (1981); J. Stöhr, and D. A. Outka, Phys. Rev. B **36**, 7891 (1987).
[38] C. Kittel, *Introduction to solid state physics* (Wiley, New York,

1966).
[39] J. Nocedal, Math. Comput. **35**, 773 (1980).
[40] J. E. Northrup, M. L. Tiago and S. G. Louie, Phys. Rev. B **66**, 121404 (2002).
[41] T. Yokoyama, K. Seki, T. Morisada, K. Edamatsu. and T. Ohta, Phys. Scr. **41**, 189 (1990); E. J. Mele, and J. J. Ritsko, Phys. Rev. Lett. **43**, 68 (1979); H. Oji, R. Mitsumoto, H. Ishi, Y. Ouchi, K. Seki, T. Yokohama, T. Ohta, and N. Kosugi, J. Chem. Phys. **109**, 10409 (1998).
[42] M. Alagia, C, Baldacchini, M. G. Betti, F. Bussolotti, V. Carravetta, U. Ekstrom, C. Mariani, and S. Stranges, J. Chem. Phys. **122**, 124305 (2005); and references therein.
[43] B. T. Thole, G. van der Laan, J. C. Fuggle, G. A. Sawatzky, R. C. Karnatak, and J. M. Esteva, Phys. Rev. B **32**, 5107 (1985), R. Nakajima, J. Stöhr, and Y. U. Idzerda, *ibid.* **59**, 6421 (1999).
[44] S. Iacobucci (private communication).
[45] M. F. Danişman, L. Casalis, and G. Scoles, Phys. Rev. B **72**, 085404 (2005).
[46] K. Lee and J. Yu, Surf. Sci. **589**, 8 (2005).
[47] M. Simeoni, S. Picozzi, and B. Delley, Surf. Sci. **562**, 43 (2004).
[48] R. Campbell, J. Robertson and J. Trotter, Acta Crystallogr. **14**, 705 (1961).